iScience

CellPress
OPEN ACCESS

Article

Deubiquitinase USP1 influences the dedifferentiation of mouse pancreatic β-cells

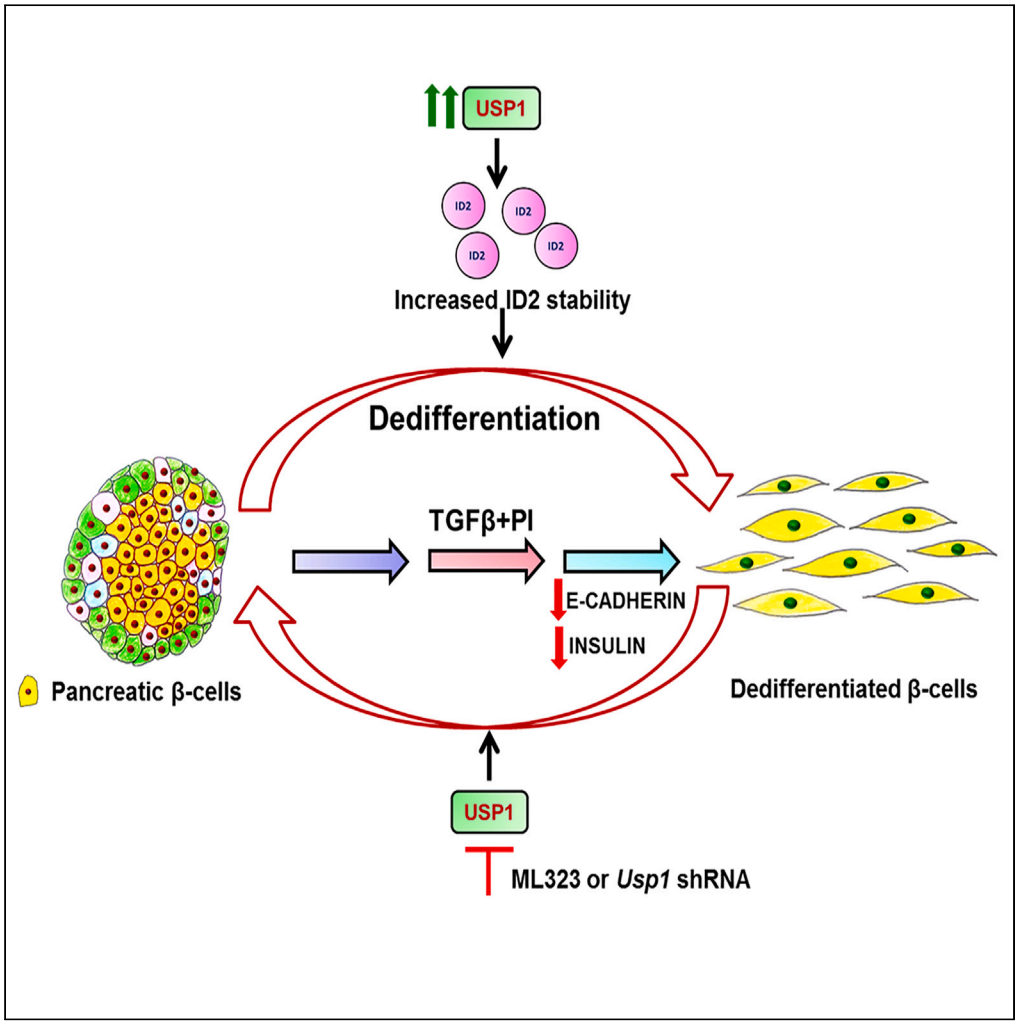

Meenal Francis, Smitha Bhaskar, Saarwani Komanduri, Preethi Sheshadri, Jyothi Prasanna, Anujith Kumar

anujith.kumar@manipal.edu

Highlights

Specific upregulation of deubiquitinase USP1 during β-cell dedifferentiation

Inhibition of USP1 inhibited dedifferentiation and rescued epithelial phenotype

Inhibition of USP1 rescues dedifferentiation induced hyperglycemia *in vivo*

ID2 is the downstream target of USP1 in enhancing the dedifferentiation

Francis et al., iScience *26*, 106771
May 19, 2023
https://doi.org/10.1016/j.isci.2023.106771

iScience

CellPress
OPEN ACCESS

Article

Deubiquitinase USP1 influences the dedifferentiation of mouse pancreatic β-cells

Meenal Francis,[1] Smitha Bhaskar,[1] Saarwani Komanduri,[1] Preethi Sheshadri,[1] Jyothi Prasanna,[1] and Anujith Kumar[1,2,*]

SUMMARY

Loss of insulin-secreting β-cells in diabetes may be either due to apoptosis or dedifferentiation of β-cell mass. The ubiquitin-proteasome system comprising E3 ligase and deubiquitinases (DUBs) controls several aspects of β-cell functions. In this study, screening for key DUBs identified USP1 to be specifically involved in dedifferentiation process. Inhibition of USP1 either by genetic intervention or small-molecule inhibitor ML323 restored epithelial phenotype of β-cells, but not with inhibition of other DUBs. In absence of dedifferentiation cues, overexpression of USP1 was sufficient to induce dedifferentiation in β-cells; mechanistic insight showed USP1 to mediate its effect via modulating the expression of inhibitor of differentiation (ID) 2. In an *in vivo* streptozotocin (STZ)-induced dedifferentiation mouse model system, administering ML323 alleviated hyperglycemic state. Overall, this study identifies USP1 to be involved in dedifferentiation of β-cells and its inhibition may have a therapeutic application of reducing β-cell loss during diabetes.

INTRODUCTION

Diabetes is a metabolic disease presented with a condition of hyperglycemia owing to the weaning of pancreatic β-cells. Autoimmune destruction of β-cells and β-cell stress due to systemic resistance to insulin are the major reasons for the loss of pancreatic β-cells.[1,2] Recent theories divulge in accounting to loss of β-cells to multiple cellular attires such as transdifferentiation and dedifferentiation.[3,4] The latest "Anna Karenina Model" suggests dedifferentiation to be a transitory fate change depending on the stage of the disease.[5] Several cell-based lucrative avenues to restore β-cells have been postulated. Transplantation of cadaver donor islets or β-cells derived from differentiation of pluripotent stem cells are ideal cell-based strategies; however, they are fraught with shortage of donors and inefficient differentiation, respectively.[6,7] These hurdles could be overcome by formulating a protocol that enhances *in vitro* differentiation or find an approach to enhance endogenous β-cell mass either by blocking transdifferentiation or dedifferentiation.

The *in vitro* culture of islet β-cells is an extremely difficult task owing to the non-proliferative disposition of islet cells and unaccountable fibroblast-like cells emerging from the islet clusters.[8–10] In a later study, serum-free cultures of β-cells indicated the ability of the cells to shuttle between functional epithelial and mesenchymal fates.[11] There have been multiple experimentally proven works including lineage tracing studies showing the dedifferentiation process to be occurring in β-cells and proved to be one of the major reason in the manifestation of diabetes.[12–15] Dedifferentiation process involves epithelial β-cells transforming to a proliferative mesenchymal cell-like phenotype with non-functional progenitor state.[5] Cellular signatures also transit from loss of mature β-cell-specific markers such as MAFA and PDX1 to transcribing forbidden genes such as NGN3 and ALDH1A3 and even pluripotent genes.[16] Molecular detailing showed transcription factor forkhead box protein O1 (FOXO1) to translocate to the nucleus under metabolic stress conditions and inhibit the matured β-cells undergoing reprograming to the progenitor state. FOXO1 also rescues key parameters related to diabetes like decreased β-cell mass and function.[14,17–19] Injury models such as pancreatic ductal ligation or pancreatectomy conditions have shown to drive the dedifferentiation of β-cells and the mechanism has been attributed to the signaling of TGFβ secreted by the immune cells.[15] Moreover, adult β-cells during this condition begin expressing epithelial-mesenchymal transition (EMT) gene Snail2.[20]

The homeostasis of transcription factors (TFs) regulating dedifferentiation is regulated either at transcriptional level or by targeting them to ubiquitin-proteasome system (UPS) or lysosomal autophagy

[1]Manipal Institute of Regenerative Medicine, Bangalore, Manipal Academy of Higher Education, Manipal, India

[2]Lead contact

*Correspondence: anujith.kumar@manipal.edu

https://doi.org/10.1016/j.isci.2023.106771

pathway.[21–27] More than 60% of cellular proteins are subjected to proteasome-mediated degradation. The UPS involves ligases (E1, E2, and E3) that facilitate various degrees of ubiquitination resulting in mono-, oligo-, or polyubiquitinated forms of proteins. In general, proteins ubiquitinated at K48 are targeted to proteasomal degradation.[28,29] In contrary, deubiquitinases (DUBs) are set of enzymes which deubiquitinate targeted proteins and thereby salvage them from proteasomal degradation.[30,31] Several events occurring during pancreatic development or dedifferentiation of β-cells are governed by the UPS. The TF PDX1 which is important for the development of pancreatic epithelial cells is targeted to proteasomal degradation by E3 ligase PDX1 C-terminus-interacting factor-1. Deletion of FBW7 ubiquitin ligase in adult pancreas drives ductal cells toward β-cells. E3 ligase Mind bomb1 targets Notch receptor Delta to proteasomal degradation and regulates the pancreatic proximal-distal axis patterning of pancreas.[32–35]

The role of DUBs in the context of dedifferentiation of cancer cells is well documented. SNAIL1, a key regulator of dedifferentiation, is stabilized in esophageal squamous cell carcinoma, breast cancer cells, and lung carcinoma cells by set of DUBs including OTUB1, DUB3, and USP37, respectively.[36–38] DUB3 has also been shown to deubiquitinate SLUG and TWIST, the other two essential regulators of dedifferentiation.[39] Recent few reports provided information on direct impact of DUBs on β-cell physiology.[40] CLEC16A-RNF41 and USP8 form a tripartite complex, wherein CLEC16A is an E3 ligase that ubiquitinates RNF41 and USP8 is the DUB that deubiquitinates RNF41. The fine-tuning of RNF41 protein level dictates the mitochondrial quality in pancreatic β-cells and facilitates insulin secretion.[41] Accumulation of toxic misfolded IAPP (Islet amyloid polypeptide) oligomers is one of the reasons behind β-cell dysfunction and this is attributed majorly to failure in deubiquitination of IAPP by UCHL1 which further results in aggregation of polyubiquitinated forms.[42] Similarly, OTUB2 has been shown to deubiquitinate TRAF6 which enhances the survival activity of NF-κB in β-cells.[43] MCPIP1 is a unique protein which possesses both DUB and RNase-like activities and is responsible in shielding β-cells from cytokine toxicity.[44] Despite these initial insights, comprehensive information about DUBs in dedifferentiation of β-cells largely remains elusive and identifying the key DUBs that regulate dedifferentiation beams to be a resilient proposition to elucidate a novel therapeutic approach.

In the present study, we aimed to investigate and identify key DUBs involved in dedifferentiation of pancreatic β-cells. Screening for DUBs revealed USP1 to be the probable candidate and loss and gain of function further reiterated the important role of USP1 in dedifferentiation. Administration of small-molecule inhibitor of USP1 in a dedifferentiation diabetic mouse model reduced the blood glucose levels and maintained the glucose tolerance test (GTT) and islet architecture near to normalcy. Finally, experiments to examine the downstream effector of USP1 revealed inhibitor of differentiation 2 (ID2) to be the downstream protein responsible for the dedifferentiation process.

RESULTS

USP1 is upregulated during dedifferentiation of pancreatic β-cells

To identify the key DUB involved in dedifferentiation of β-cells, we generated *in vitro* dedifferentiation model system by subjecting MIN6 cells to TGFβ and proteasomal inhibitor (PI) treatment.[45,46] The cells showed reduced epithelial marker *E-Cadherin* and a corresponding decrease in *insulin* and a moderate increase in mesenchymal marker Snail1 at the transcript level (Figure S1A). Flow cytometry and Western blot confirmed the observation by showing reduced levels of E-CADHERIN and PDX1 levels (Figure S1B and S1C), cumulatively exhibiting a dedifferentiated state. In this model system, the expression level of multiple DUBs was analyzed and identified an increased expression of *Usp1* compared to other DUBs (Figures 1A and 1B). To confirm the observation, the transcript analysis was performed along with other DUB *Usp30* and observed an enhanced expression of *Usp1*, but not the *Usp30*, in TGFβ +PI-treated condition compared to untreated cells (Figure 1B). The upregulation of USP1 was consistent at the protein level as observed by flow cytometry analysis (Figure 1C). Mimicking the hyperglycemic condition, MIN6 cells exposed to higher glucose concentration showed decreased insulin expression and in parallel increased expression of USP1 (Figures S1D and S1E). To validate the elevated expression of USP1 in a dedifferentiated condition, we isolated primary islets from the mice and authenticated the identity of insulin-producing cells by DTZ staining, immunofluorescence of C-peptide (Figures S2A, S2B and S2C), and transcript analysis of *Insulin*, *Nkx6.1*, and *E-Cadherin* (Figure S2D). The primary islets cultured on fibronectin-coated dish displayed the emanating fibroblast-like cells from the islets (Figure S3A) and transcript analysis showed downregulation of pancreatic matured β-cell-specific markers *Insulin*, *Nkx6.1*, *Pdx1*, and epithelial marker *E-Cadherin* and increased expression of mesenchymal markers *Snail1*, *Snail2*, and *Twist* compared to

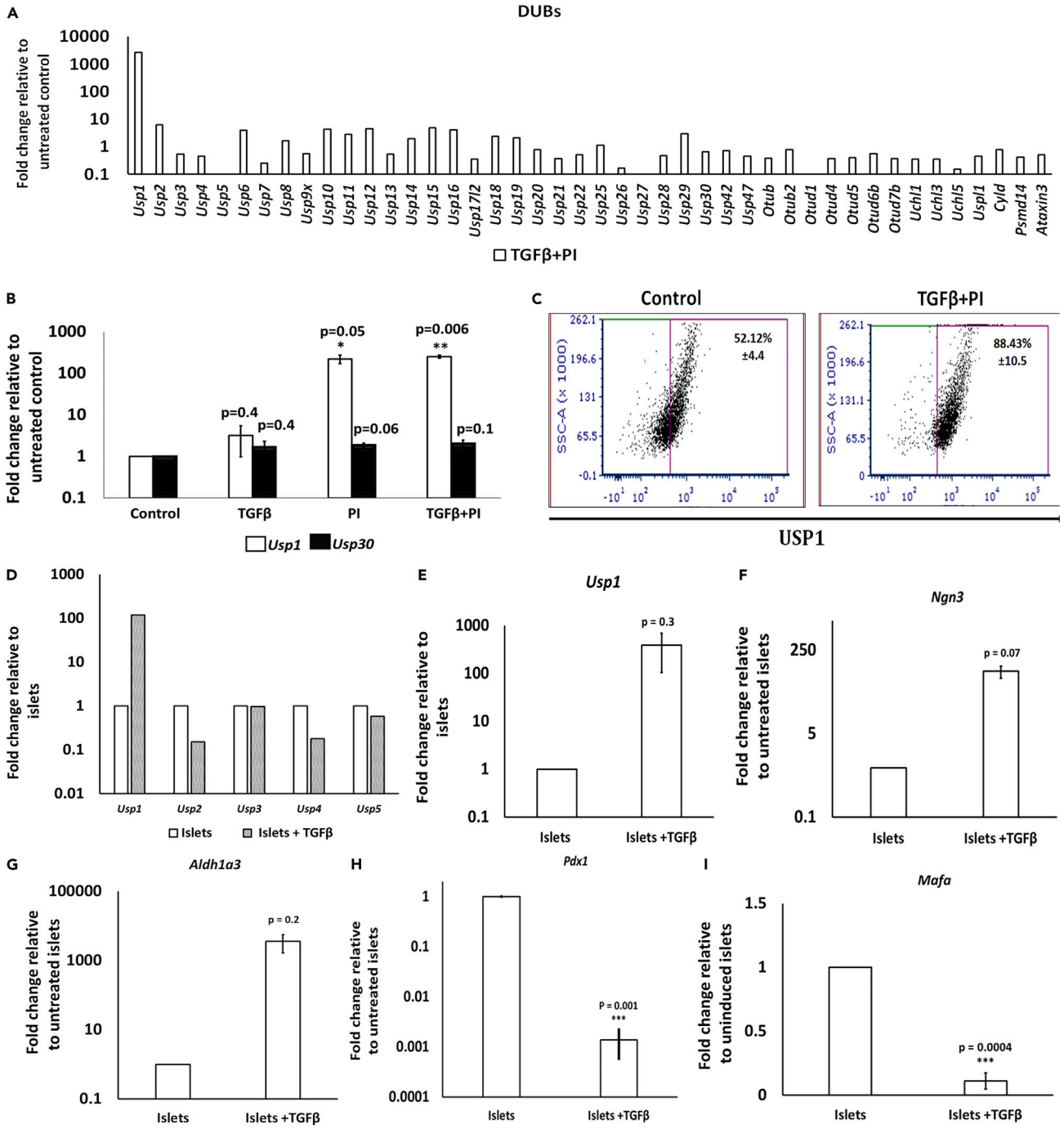

Figure 1. Enhanced expression of USP1 upon mesenchymal transition of pancreatic β cells

(A) MIN6 cells treated with TGFβ+PI were screened for expression of DUBs. Transcript analysis for the expression of various DUBs in MIN6 based model of dedifferentiation compared to untreated control highlighting the expression of USP1.

(B) Transcript analysis of *Usp1* and *Usp30* in MIN6 cells treated with TGFβ, PI and TGFβ +PI.

(C) Dot plots representing flow cytometry analysis for expression of USP1 in MIN6 cells treated with TGFβ+PI compared to control.

(D–G) Transcript analysis for the expression of β-cell progenitor genes *Ngn3* and *Aldh1a3* and mature genes *Mafa* and *Pdx1* in mouse islet cells treated with TGFβ compared to untreated control.

(H) Transcript analysis of expression of representative DUBs in *in vitro* TGFβ-treated mouse islets compared to untreated control.

(I) Transcript analysis of expression of USP1 in endogenous mouse islets treated with TGFβ compared to untreated islets. Data represented as mean ± S.E.M. of 3 sets of experiments *p < 0.05 and **p < 0.01. All Ct values of RT-PCR data are normalized to housekeeping gene *Gapdh*.

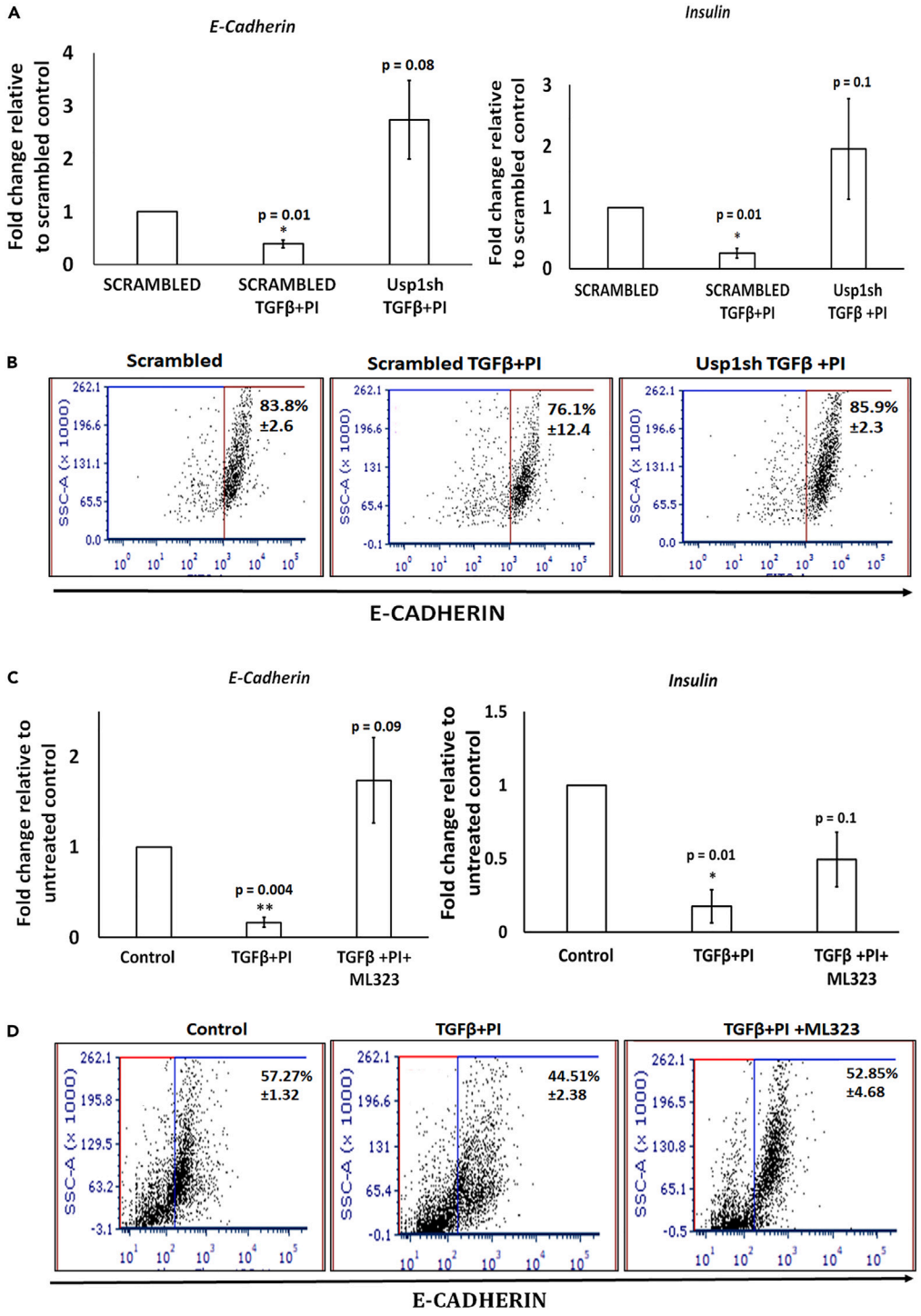

Figure 2. Inhibiting USP1 reverses TGFβ+PI-mediated dedifferentiation

(A) MIN6 cells transduced with USP1 shRNA were treated with TGFβ+PI and analyzed at the transcript level for *Insulin* and *E-Cadherin*.

(B) Flow cytometry analysis for the expression of E-CADHERIN in MIN6 cells treated TGFβ+PI in presence of USP1 shRNA compared to scrambled controls.

(C)Transcript analysis of *E-Cadherin* and *Insulin* expression in cells treated with TGFβ+PI + ML323.

Figure 2. *Continued*

(D) Dot plots representing flow cytometry analysis for the expression of E-CADHERIN in cells treated with TGFβ+PI + ML323 or TGFβ+PI compared to untreated control. Data represented as mean ± S.E.M. of 3 sets of independent experiments *$p < 0.05$ and **$p < 0.01$. All Ct values of RT-PCR data are normalized to housekeeping gene *Gapdh*.

the isolated islets (Figures S3B and S3C). However, they lacked the expression of *Usp1* (Data not shown). Subjecting the primary islets to TGFβ treatment showed upregulated expression of *Usp1*, but not the other DUBs, similar to that observed in MIN6 cells treated with TGFβ+PI (Figures 1D and 1E). In corroboration with the key feature of dedifferentiation process as to lose the expression of mature β-cell-specific markers and increase the transcription of forbidden genes, we observed enhanced expression of progenitor genes *Ngn3* and *Aldh1a3* and decreased expression of matured genes *Pdx1* and *Mafa* (Figures 1F–1I). These results signify a strong correlation between USP1 and dedifferentiation process in β-cells.

USP1 expression is essential for the dedifferentiation of MIN6 cell line

In order to explore the role of USP1 in the dedifferentiation process, we knocked down the expression using USP1-specific short hairpin RNA (shRNA). The USP1 shRNA efficiently inhibited the expression of USP1 which was monitored at the transcript level (Figures S4A and S4B) as well at the protein level (Figure S4C). Treatment of MIN6 cells with TGFβ+PI and transduced with scrambled shRNA showed 70% reduction in the expression of *E-Cadherin* and 76% reduction in *Insulin* expression at transcript level as assayed by qPCR and E-CADHERIN expression at protein level as analyzed by the flow cytometry (Figures 2A and 2B). Interestingly, transduction of these cells with USP1-specific shRNA showed significant rescue in the expression of *E-Cadherin* and *Insulin* at transcript level and E-CADHERIN at protein level (Figures 2A and 2B). Supporting the observation, compared to TGFβ+PI-treated cells, there was 30% reduction in expression of mesenchymal gene VIMENTIN in cells transduced with USP1 shRNA (Figure S5). However, similar inhibition of USP30 using USP30 shRNA lacked the ability to rescue the expression of E-CADHERIN, denoting the specificity of USP1 in the dedifferentiation process (Figure S6). In parallel, similar rescue effect was observed in *in vitro* dedifferentiated mouse primary islets as represented by transcript analysis for the expression of *E-Cadherin* and *Insulin* under conditions of USP1shRNA-transduced cells (Figure S4D). Previous studies showed USP1 activity could be allosterically inhibited using small-molecule ML323.[47] Inhibition of USP1 using ML323 in TGFβ+PI-treated dedifferentiated MIN6 cells displayed a rescue in the transcript of *E-Cadherin* and *Insulin* at transcript level (Figure 2C) and increased expression of E-CADHERIN and decreased expression of VIMENTIN at protein level (Figures 2D, and S7B). Similar treatment of ML323 in TGFβ-treated *in vitro* dedifferentiated mouse primary islets showed rescue in the expression of E-cadherin and insulin (Figure S7B). Previous studies had shown the mesenchymal cells emanating from the cultured mouse islets to have the ability to redifferentiate back into islet-like clusters when cultured in low adherent condition.[48] To further understand the advantage of inhibiting USP1 in redifferentiation, MIN6 cells were subjected to sphere formation and observed decreased sphere size, sphere count, and *E-Cadherin* mRNA expression in presence of TGFβ+PI and all the said parameters were rescued upon inhibition of USP1 (Figures S8A–S8D). Compared to monolayer, there was increase in INSULIN-positive cells in MIN6 spheres, but upon inhibition of USP1 by ML323 there was 4-fold further increase in *Insulin* transcript and ~2-fold increase in E-CADHERIN protein compared to spheres (Figures S8E–S8H). Overexpression of USP1 in spheres also decreased the expression of *E-Cadherin* transcript which was rescued by inhibiting USP1 by ML323 (Figure S8I). These results indicate the essential role of USP1 in the dedifferentiation of pancreatic β-cells.

Overexpression of USP1 is sufficient to induce dedifferentiation of MIN6 cells

To further confirm the role of USP1 in dedifferentiation of pancreatic β-cells, we analyzed the dedifferentiation process in a USP1-overexpressed state. For this, MIN6 cells were transduced with a doxycycline-inducible USP1 overexpression construct which upon addition of doxycycline showed enhanced expression of *Usp1* (Figure S9A). Overexpression of USP1 was sufficient to reduce the expression of matured β-cell genes *E-Cadherin*, *Insulin*, *Pdx1*, and *Mafa* and concomitantly increased expression of progenitor genes *Ngn3* and *Aldh1a3* and mesenchymal gene *Snail2* at transcript level (Figures 3A–3E and Figure S9B). Decreased expression of PDX1 and INSULIN and increased expression of ALDH1A3 was observed at protein level as assayed by flow cytometry (Figures 3F–3J) and immunofluorescence (Figure 3K). To confirm the endogenous expression of progenitor gene NGN3 in MIN6 cells during the course of dedifferentiation, we transduced the *Ngn3::GFP* construct, wherein the expression of GFP indicates the *Ngn3* promoter activity.

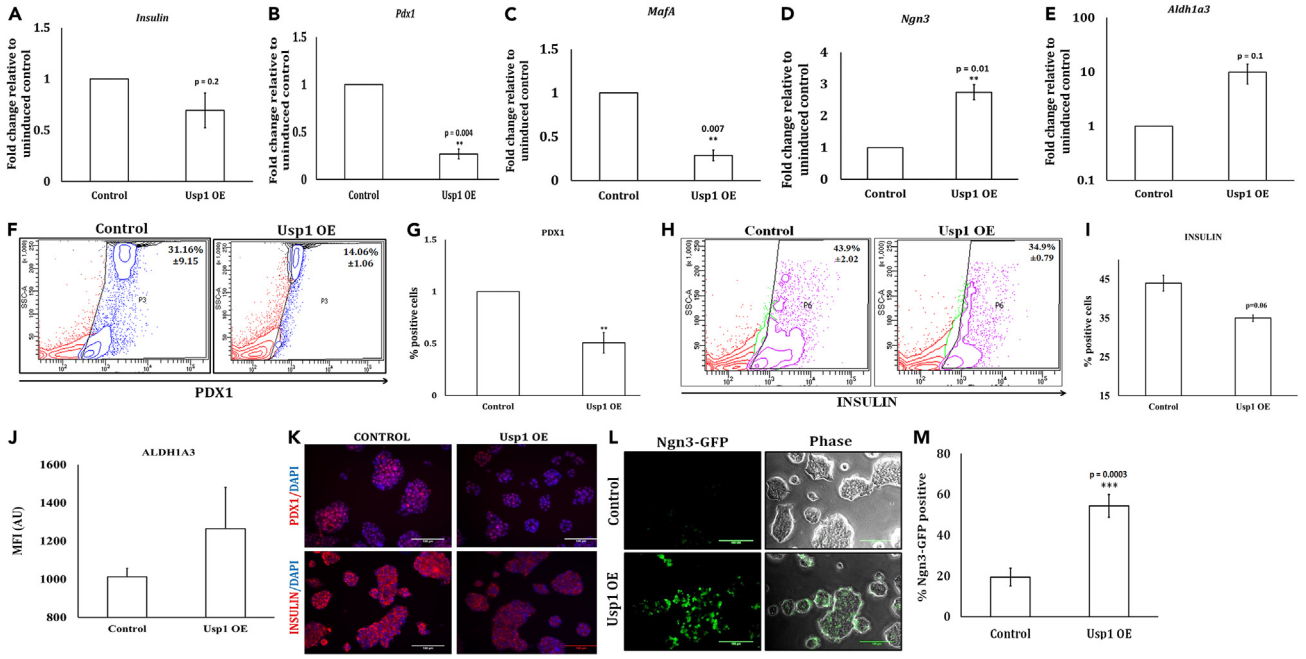

Figure 3. Overexpression of USP1 is sufficient to induce dedifferentiation of MIN6 cells

(A–E) Transcript analysis for the expression of β-cell-specific mature markers *Insulin*, *Pdx1*, and *Mafa* and progenitor markers *Ngn3* and *Aldh13a* in MIN6 cells transfected with doxycycline-induced USP1 overexpression construct compared to uninduced counterparts. Data represented as mean ± S.E.M. of 3 independent experiments. *p < 0.05 and **p < 0.01. All Ct values of RT-PCR data are normalized to housekeeping gene *Gapdh*.

(F–J) Flow cytometry analysis and its quantification graph for the protein expression of PDX1 (F and G) and INSULIN (H and I) in MIN6 cells overexpressing USP1 and compared to cells untreated with doxycycline. (J) Mean fluorescence intensity obtained from flow cytometry analysis for protein ALDH1a3 in MIN6 cells overexpressing USP1 and compared to cells untreated with doxycycline.

(K) Fluorescence images of MIN6 cells transfected with doxycycline-induced USP1 overexpression construct compared to uninduced counterparts probed with Pdx1 and Insulin antibodies.

(L–M) Fluorescent and phase contrast image of MIN6 cells harboring *Ngn3* promoterGFP construct and doxycycline-inducible USP1 overexpression construct. Increased GFP-positive cells denoting the increased expression of NGN3 is observed in cells overexpressing USP1 and the percentage positive GFP cells are quantified in (M). Data represented as mean ± S.E.M. of 3 sets of experiments *p < 0.05 and **p < 0.01. Scale bar 100 μM.

Compared to control, overexpression of USP1 showed increased GFP expression, indicating increased *Ngn3* promoter activity (Figures 3L and 3M).

To reiterate the specificity of the USP1's contribution in the dedifferentiation process, USP1 was overexpressed in USP1 shRNA background and analyzed for the expression of epithelial genes. Compared to untreated control, TGFβ+PI-treated cells showed 2-fold decrease in the expression of *E-Cadherin* at transcript level and 13% decrease at protein level. Transduction of USP1 shRNA in this condition rescued the expression of *E-Cadherin* and showed 6-fold increase in expression at transcript level and 12% increased expression at protein level compared to TGFβ+PI-treated cells. Overexpression of USP1 in USP1 shRNA background significantly decreased the expression of E-CADHERIN both at transcript and protein level (Figures 4A, 4B, and 4C). To strengthen the observation, instead of shRNA we performed similar experiment in presence of ML323 and observed rescue in the expression of *E-Cadherin* at transcript level and protein levels in cells treated with TGFβ+PI and ML323 in comparison to cells treated with TGFβ+PI alone. Overexpression of USP1 in ML323-treated cells significantly reduced the expression of E-CADHERIN and maintained the expression similar to that of TGFβ+PI-treated condition (Figures 4D, 4E, and 4F). These results indicate that the increased dedifferentiation observed in β-cells is the consequence of specific upregulation in the expression of USP1 protein.

In vivo inhibition of USP1 reversed hyperglycemia in STZ-induced diabetic mouse model

Extending the study to an *in vivo* β-cell dedifferentiation model, we followed the protocol designed by Sachs et al., 2020, wherein β-cell dedifferentiation was established by administering mice with

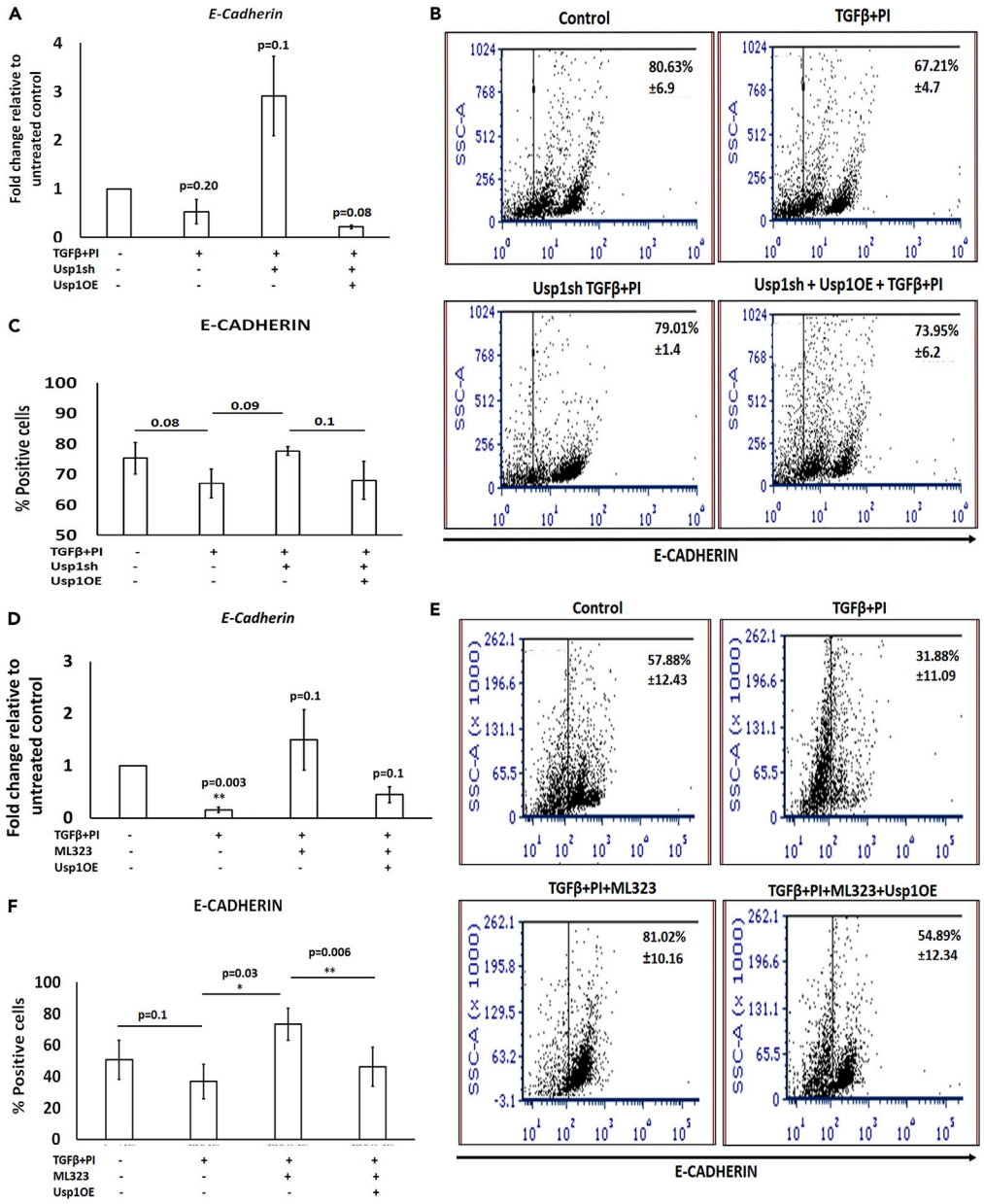

Figure 4. Overexpression of USP1 facilitates dedifferentiation of MIN6 cells

(A)Transcript analysis of *E-Cadherin* in USP1sh and USP1-overexpressed cells treated with TGFβ+PI compared to untreated control.

(B) Flow cytometry analysis of E-CADHERIN in USP1sh and USP1-overexpressed cells treated with TGFβ+PI and compared to untreated control.

(C) Quantitative representation of flow cytometry analysis of E-CADHERIN expression shown in panel b.

(D) Transcript analysis for the expression of *E-Cadherin* in ML323 and USP1-overexpressed cells treated with TGFβ+PI compared to untreated control.

(E) Flow cytometry analysis of expression of E-CADHERIN in ML323 and USP1-overexpressed cells treated with TGFβ+PI compared to untreated control.

(F) Quantitative representation of flow cytometry analysis of E-CADHERIN expression shown in panel e. Data represented as mean ± S.E.M. of 3 sets of independent experiments *p < 0.05 and **p < 0.01. All Ct values of RT-PCR data are normalized to housekeeping gene *Gapdh*.

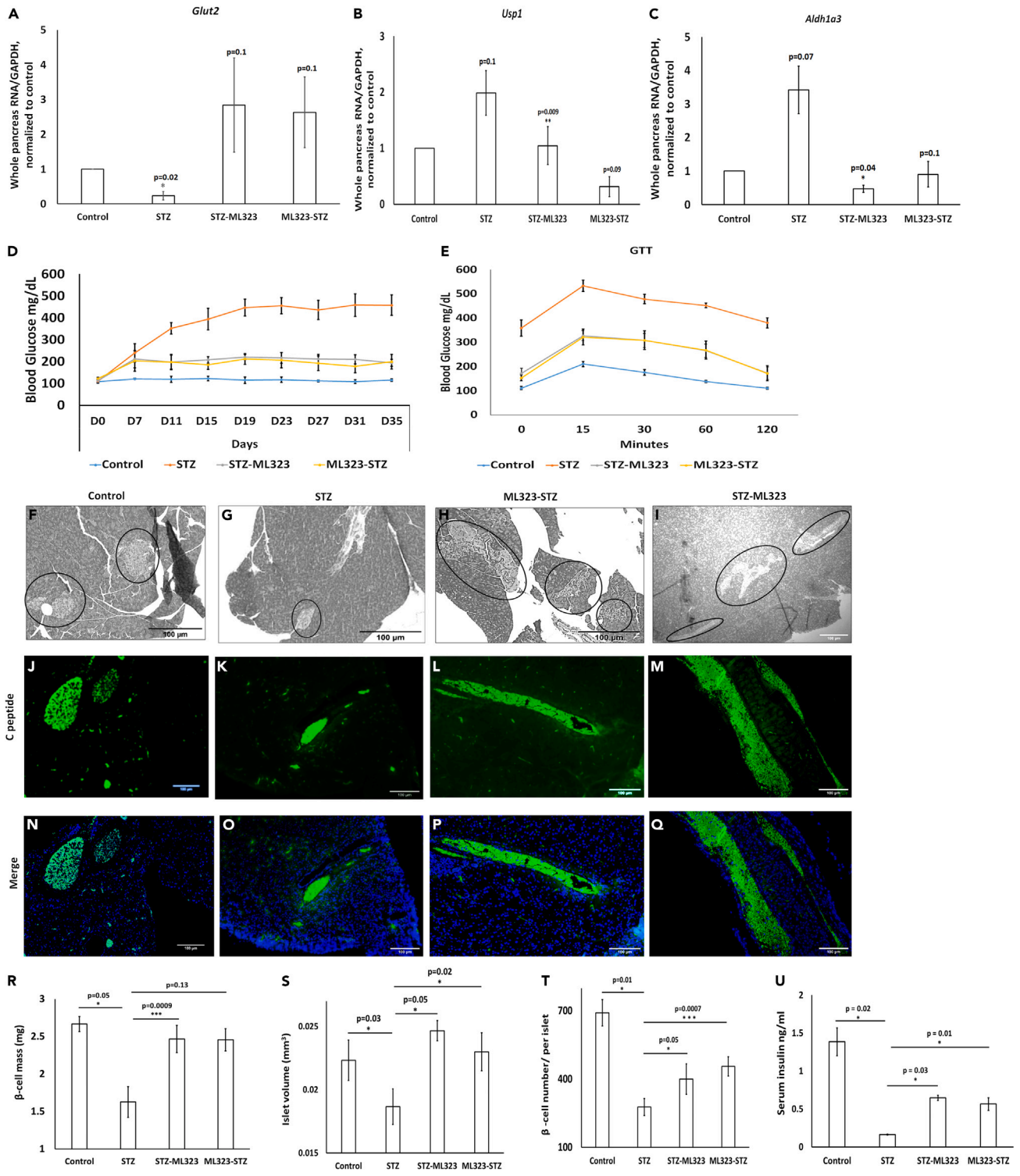

Figure 5. USP1 inhibitor ML323 rescues hyperglycemia in STZ induced diabetic mice model

(A–C) Transcript analysis for the expression of Glut2, USP1 and Aldh1a3 in the pancreas of STZ and ML323 treated animals compared to untreated control animals. Data represented as mean ±S.E.M. of 3 sets of experiments.

(D) Graph representing blood glucose levels across day points of diabetic animals treated with STZ and ML323 compared to untreated animals (N=5).

(E) Blood glucose levels measured upon glucose tolerance test on day 30 of diabetic animals treated with STZ and ML323 compared to untreated animals (N=5).

Figure 5. *Continued*

(F–I) Haematoxylin and eosin stained sections of pancreatic tissue derived from STZ (G), ML323 injected 3 days prior to STZ treatment (ML323-STZ) (H) and ML323 injected 3 days after STZ treatment (STZ-ML323) (I) animals compared to untreated animals (F).

(J–Q) Immunohistochemical analysis of C-peptide in pancreatic sections obtained from diabetic animals treated with ML323 (L and M) and untreated diabetic (K) and normal control (J) with respective merge images (N–Q).

(R–U) Graphs representing islet β-cell mass (R), volume (S) and β-cell numbers per islet (T) obtained from sections of pancreas from diabetic mice treated with ML323 compared to untreated diabetic and normal control. (U) Graph representing ELISA for serum insulin levels of diabetic mice treated with STZ and ML323 treated animals compared to untreated control animals.

Data represented as mean ±S.E.M. of 3 sets of experiments. *p <0.05, **p < 0.01 and ***p <0.001. All Ct values of RT-PCR data are normalized to housekeeping gene GAPDH.

intraperitoneal injections of streptozotocin (STZ) for 6 consecutive days. In the mice experiments, the following experimental set up was formulated: a) control mice N = 5, b) STZ mice N = 5, c) ML323 treatment prior to STZ injection N = 5 mice, and d) ML323 treatment after STZ injection N = 5 mice. Transcript analysis of pancreas in STZ mice showed increased expression of *Usp1* and forbidden gene *Aldh1a3* and decreased expression of glucose transporter isoform *Glut2*. The mice treated with USP1 inhibitor either prior or after STZ treatment showed decreased expression of *Usp1* and *Aldh1a3* and rescued the expression of *Glut2* (Figure 5A,5B, and 5C). Blood glucose levels were monitored on alternate day points up to day 35. Blood glucose of mice treated with STZ showed an average of 400–500 mg/dl. Interestingly, the mice treated with ML323 either 3 days before or 3 days after STZ injection showed reduced blood glucose level with an average of 200–250 mg/dl (Figure 5D). An intraperitoneal GTT was performed after 30 days in mice that received ML323 and observed better clearance of glucose compared to STZ-treated and ML323-untreated mice (Figure 5E). Histology of the pancreas of diabetic mice treated with ML323, untreated diabetic, and normal animals was analyzed by H&E staining and immunohistochemical staining for c-peptide. H&E (Figures 5F–5I) and immunohistochemical staining (Figures 4J–4Q) studies showed rescue in islet architecture in pancreatic sections of mice treated with ML323 compared to STZ-treated mice. Similar rescue in β-cell mass, islet volume, and β-cell number/islet was observed in mice treated with ML323 (Figure 5R–5T). Estimation of serum insulin showed reduced insulin amount in STZ-treated mice compared to control whereas treatment with ML323 either prior or after STZ treatment showed ∼3-fold rescue in serum insulin amount compared to STZ mice (Figure 5U). Clustering the entire observation, we propose that diabetic animals treated with ML323 sustain functionality of β-cells in the prevailing diabetic conditions probably by inhibiting dedifferentiation.

ID2 is the downstream effector of USP1-mediated dedifferentiation of β-cells

In the prospects of understanding the underlying mechanism of USP1-mediated dedifferentiation of β-cells, we sought after the available information in the literature and found ID family proteins to be the substrates of USP1 in certain metastatic conditions.[49,50] This intrigued us to investigate whether ID2 participates in the USP1-mediated dedifferentiation process in the β-cells. Analysis at the transcript level for the expression of ID family genes, ID1, ID2, and ID3, in islet cells treated with TGFβ compared to untreated controls revealed the upregulation of ID2 compared to ID1 and ID3 (Figure 6A). Furthermore, we looked into the expression of ID2 genes in a USP1-inhibited condition and found islets transduced with USP1sh RNA and treated with TGFβ showed ID2 to be highly downmodulated (Figure 6B). This indicated ID2 protein to be responding to the modulation in USP1 expression level. To analyze whether the stability of ID2 is determined by USP1, we overexpressed USP1 in MIN6 cells cultured in presence or absence of translational inhibitor cycloheximide and found ID2 protein to be stabilized in cells overexpressing USP1 compared to vector control (Figure 6C). The stability of ID2 was further corroborated by decreased expression of *NeuroD* transcript in cells overexpressing USP1 and the inhibition being reversed by inhibiting USP1 (Figures 6D and 6E). *NeuroD* has been shown to be the direct downstream target and being repressed by ID2 protein.[51]

To further reveal whether ID2 to be the downstream effector of USP1 in regulating the dedifferentiation process, we strategized to perform ID2 loss and gain of function in presence or absence of USP1 in MIN6 cells. Overexpression of ID2 in cells cultured in presence of TGFβ+PI reduced the expression of *E-Cadherin* by 2-fold at transcript level and by 12% at protein level compared to TGFβ+PI-treated cells (Figure 7 a-c). Inhibition of ID2 expression by ID2-specific shRNA reversed the TGFβ+PI-mediated reduced expression of *E-Cadherin* and dedifferentiation process. There was ∼3.2-fold increase in the expression of *E-Cadherin* at transcript level and ∼8% increase at protein level compared to TGFβ+PI-treated scrambled control (Figure 7 d-f). To correlate the relation between USP1 and ID2, we knocked down ID2 in

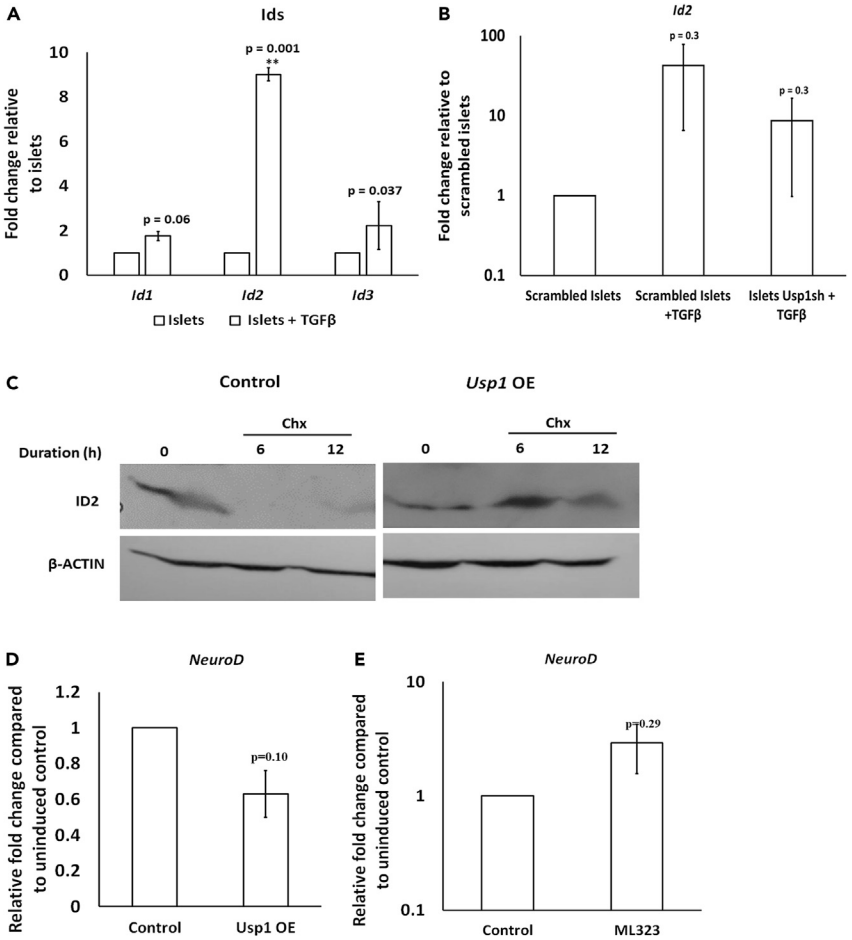

Figure 6. Overexpression of USP1 stabilizes ID2

(A) Transcript analysis for ID family genes in TGFβ-treated dedifferentiated islets compared to untreated counterpart.

(B) Transcript analysis for the expression of *Id2* in presence of USP1sh RNA in islets treated with TGFβ compared to scrambled control.

(C) Immunoblot of ID2 in MIN6 cells overexpressing USP1 and treated with cycloheximide for different hours. β-actin blot is used as protein loading control. Transcript analysis of *NeuroD*, the downstream target of ID2, in MIN6 cells either overexpressing USP1.

(D) or treated with USP1 inhibitor ML323.

(E) Data represented as mean ± S.E.M. of 3 sets of independent experiments, *$p < 0.05$ and **$p < 0.01$. All Ct values of RT-PCR data are normalized to housekeeping gene *Gapdh*.

presence of USP1 overexpression condition and analyzed for the expression of E-CADHERIN in MIN6 cells. In cells overexpressing USP1, ~ 2-fold decrease in the expression of *E-Cadherin* at a transcript level and 22% at protein level compared to vector control was observed. Inhibition of ID2 in this USP1 overexpression condition by transducing ID2-specific shRNA reversed the expression of *E-Cadherin* by ~4.5-fold at transcript level and 18% at protein level compared to USP1 overexpression and scrambled shRNA-transduced condition (Figure 7 g-i). In conclusion, these experiments reveal the activation of USP1 during dedifferentiation process to coincide with ID2 expression and indicate the likeliness of ID2 being a downstream effector of USP1 during β-cells dedifferentiation.

DISCUSSION

Dedifferentiation is a cardinal process playing a dogmatic role during pancreatic β-cell development as well in metabolic diseases like diabetes.[14,52,53] Several experimental evidences showed the occurrence of β-cell dedifferentiation which could be one of the major reason for depleted mass in hyperglycemic

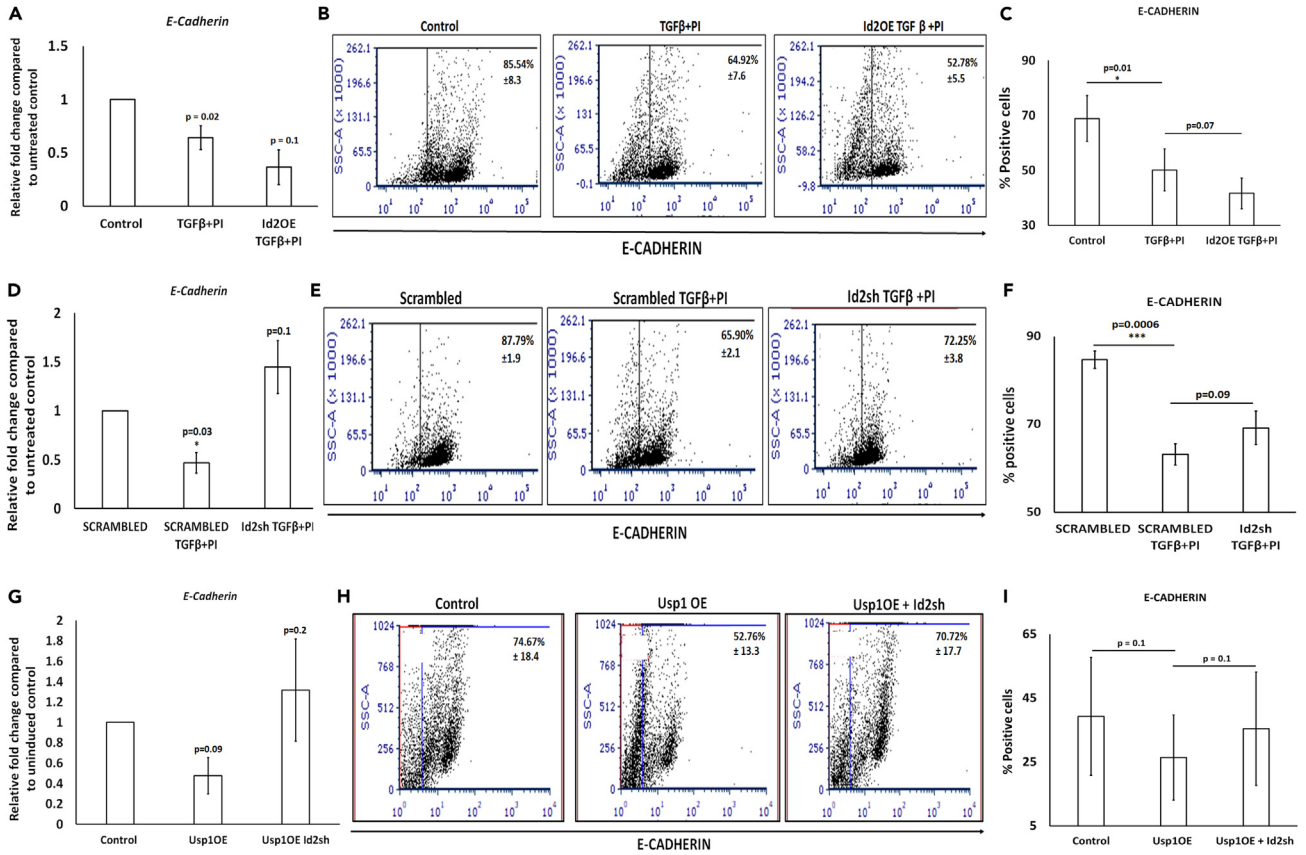

Figure 7. Inhibition of ID2 rescues the USP1-mediated dedifferentiation of β-cells

(A) Transcript analysis of the expression of *E-Cadherin* in MIN6 cells transfected with ID2-overexpressing construct and treated with TGFβ+PI compared to vector transfected and untreated control.

(B) Flow cytometry analysis for the expression E-CADHERIN in MIN6 cells harboring ID2 overexpression construct or vector alone control treated with TGFβ+PI and compared with untreated controls.

(C) Graphical representation of the flow cytometry analysis indicating percentage positive cells in panel b. Transcript.

(D and E) and flow cytometry (E) analysis for the expression of E-CADHERIN in MIN6 cells transduced with ID2shRNA and treated with TGFβ+PI compared to scrambled TGFβ+PI-treated and scrambled untreated controls.

(F–H) Graphical representation for the flow cytometry analysis indicating percentage positive cells of panel e. Transcript (G) and flow cytometry (H) analysis for the expression of E-CADHERIN in MIN6 cells transduced with ID2shRNA in a USP1 overexpression background treated with TGFβ+PI compared to USP1 OE alone and vehicle control.

(I) Graphical representation for the flow cytometry analysis indicating percentage positive cells of panel h. Data represented as mean ± S.E.M. of 3 sets of experiments *p <0.05 and **p < 0.01. All Ct values of RT-PCR data are normalized to housekeeping gene *Gapdh*.

state.[54,55] Retaining *in vivo* β-cell mass by avoiding dedifferentiation is an ideal alternative strategy to combat β-cell loss. In the present study, we investigated the role of DUB USP1 and observed its role in *in vitro* and *in vivo* dedifferentiation of pancreatic β-cells. Inhibition of USP1 facilitated in retaining the epithelial phenotype and thereby properties of β-cell. Attempts to understand the mechanism shed light on ID2 to be the probable downstream substrate of USP1 during this process. The outcome of the present study helps in better understanding the process of dedifferentiation in β-cells and small-molecule-mediated inhibition of USP1 takes a step closer to sustain the β-cell mass.

Several studies showed various signaling pathways to participate in the dedifferentiation process. Recent study by Xiao et al. showed the TGFβ secreted by M2 macrophages to be responsible for the dedifferentiation process of β-cells in a ductal ligated mouse model system.[15] Due to lesser number of DUBs being encoded by mouse genome compared to E3 ligases, screening for DUBs in dedifferentiation process proved more feasible. Considering the evidence of TGFβ in dedifferentiation, we dedifferentiated MIN6 cells line by treating with TGFβ and PI and screened for key DUBs based on their expression level. We

detected the transcript levels of *Usp1* to be highly upregulated compared to other DUBs. Furthermore, enhanced expression of USP1 was also observed in primary β-cells treated with TGFβ. Several DUBs have been identified to enhance the downstream TGFβ activity by stabilizing the intermediates of TGFβ pathway. Interestingly, the deubiquitinase enzyme FAM/USP9X stabilizes Smurf1, the downstream of TGFβ cascade, and facilitates in enhancing the TGFβ activity.[56] However, in our screening process, we failed to detect the enhanced expression of any other DUBs other than USP1. Inhibition of USP1 either by shRNA or by small-molecule ML323 showed similar effect on dedifferentiation process. Previous studies had shown ML323 to inhibit the enzymatic activity of USP1 allosterically.[47,57] However, in our present study, we consistently observed the downregulation of USP1 expression at transcript and protein levels also when the cells were treated with ML323. This decrease in *Usp1* transcript could be probably a secondary effect caused due to the induction of dedifferentiation process rather than the direct effect of ML323 on the transcription of *Usp1* expression. There are a few recent reports which showed a direct correlation between USP1's activity and manifestation of β-cell failure. Inhibition of USP1 was shown to protect β-cells from glucose toxicity-induced apoptosis and the mechanistic insights showed USP1 inhibition to enhance the DNA damage response and in turn to facilitate the β-cell survival.[58] In our study, though we failed to find difference in β-cell survival upon overexpression or inhibition of USP1, our experimental results indicate inhibition of dedifferentiation in USP1 knockdown condition to be the other alternative mechanism involved in retaining β-cell function.

To date, there has been an ongoing debate on whether β-cells per se undergo dedifferentiation or the mesenchymal cells exist from the pre-existing mesenchymal cells or is it the transdifferentiation of other islet cells.[59] Though the ambiguity persists until date, several lineage tracing studies including the elegant study by Talchai et al. showed the β-cell-specific knockout of FOXO1 to result in dedifferentiation of β-cells that results in diabetes.[14] Similarly, Mak et al. demonstrated β-cell dedifferentiation to be part of EMT and indicated miR-7 to be the key player in enhancing the expression of mesenchymal genes leading to EMT.[60] All this collective information portrayed dedifferentiation process to exist in β-cells which triggers loss of β-cell mass and imply to be one of the major causatives of diabetes. Interestingly, in our both *in vitro* and *in vivo* model system, we observed the enhanced expression of forbidden genes and decreased expression of matured β-cell genes, authenticating the dedifferentiation process. Though we observed the occurrence of dedifferentiation in primary islet cells, we hesitate to rule out the contribution of other cells of the islets to participate in this process, as our analysis considered the entire pool of dedifferentiated cells emanating from the cultured islets and not from the fractionated homogeneous β-cells. Since larger part of islets is populated with β-cells (60%–70%), we still strongly consider the role of USP1 in the process of dedifferentiation of β-cells. To conclusively ascertain the role of USP1 in dedifferentiation, we adapted an *in vivo* diabetic dedifferentiation model system. Sachs et al. demonstrated that STZ-induced diabetes model could be utilized to study β-cell dedifferentiation in mice.[61] In the present study, in STZ-treated pancreas, there was increased expression of the pancreatic progenitor gene *Aldh1a3* along with *Usp1*. Administration of USP1 inhibitor ML323 in STZ-induced dedifferentiation model system reversed partially the hyperglycemic state and β-cell mass and number of islet-positive cells compared to STZ alone-treated mice. The islet architecture as well the insulin secretion in serum of diabetic mice treated with ML323 showed similar phenotype to that of non-diabetic controls but the untreated diabetic animals showed regressed islet clusters and reduced serum insulin. These results convincingly portrayed the significant role of USP1 in *in vitro* and *in vivo* dedifferentiation of β-cells.

Mechanistically, dedifferentiation is controlled by several transcription factors. For instance, hypoxia-inducible factor-1α has been shown to facilitate dedifferentiation of β-cells.[62] Conditional knockout of FOXO1 TF resulted in dedifferentiation of β-cells and has been shown to be the major cause of β-cell failure in type II diabetes.[14] During unfavorable dedifferentiation inducing conditions, FOXO1 translocates to the nucleus and protects the β-cells by facilitating the expression of matured markers NEUROD1 and MAFA.[17] The other important TFs family that regulates dedifferentiation process is ID family members. Elevated ID proteins are observed in several dedifferentiated primary human malignancies including pancreatic carcinoma and neuroblastomas.[63,64] There are various DUBs which regulate the homeostasis of several proteins that dictate the degree of dedifferentiation process. For instance, homeostasis of NGN3, the TF that ear marks islet precursor cells, has been shown to be dependent on the presence of NOTCH signaling.[65] DUB USP9x stabilizes the components of NOTCH and thereby increases NGN3 activity which in turn probably increases the dedifferentiation process.[66] An independent study also showed the expression of SNAIL in NGN3-expressing precursor cells which inhibited the maturation to β-cells and in parallel facilitated the

dedifferentiation process.[19] Recent study in an independent cellular system showed USP1 to deubiquitinate SNAIL1 and enhance its stability.[67] In the present study, with the goal of identifying the mechanism by which USP1 executes its role in dedifferentiation, we considered the previously available information from literature which showed the deubiquitination of ID proteins by USP1 to be essential for maintenance of mesenchymal phenotype in osteosarcoma cells[48] (Williams et al., 2011). In the process of testing whether the similar mechanism holds true in dedifferentiation of β-cells, we observed enhanced expression of ID2 compared to other ID family members in dedifferentiated MIN6 cells. Overexpression of ID2 was sufficient to induce the dedifferentiation of MIN6 cells even in absence of USP1, and inhibition of ID2 even in USP1 overexpression condition was adequate to retain the epithelial gene expression. These results indicated ID2 to be the probable downstream candidate of USP1 and deubiquitination of which probably enhances dedifferentiation of β-cells.

Endogenous β-cells undergoing dedifferentiation-mediated changes in *in vitro* culture has crippled the long-term expansion of β-cells. Therefore, it is prudent to have a better understanding of the dedifferentiation process in context of β-cells to retain functional cells in *in vitro* as well for *in vivo* therapeutic applications. Considering the outcome of the present study, altering USP1 activity could be envisaged as an alternative means to sustain *in vitro* β-cell culture as well to inhibit the *in vivo* β-cell loss in diseased state.

Limitations of the study

There are certain limitations in the study. Though we elegantly deciphered the role of USP1 in dedifferentiation using MIN6 cell line and primary β-cells, the role could be more affirmatively addressed by conditional knockout of USP1 in β-cells. In the *in vivo* diabetic model of dedifferentiation, we did demonstrate the reversal of hyperglycemia along with β-cell mass and serum insulin secretion. However, an in-depth *in vivo* characterization of the reversal of diabetes which includes the parameters like glucose-stimulated insulin secretion in the diabetic mice treated with USP1 inhibitor has not been addressed.

STAR★METHODS

Detailed methods are provided in the online version of this paper and include the following:

- KEY RESOURCES TABLE
- RESOURCE AVAILABILITY
  - Lead contact
  - Materials availability
  - Data and code availability
- EXPERIMENTAL MODEL AND SUBJECT DETAILS
  - Animals
  - Cell culture
- METHOD DETAILS
  - Mouse endogenous islet isolation
  - Blood glucose tests
  - Glucose tolerance test (GTT)
  - STZ mouse diabetic model and ML323 treatment
  - Transfection and transduction
  - Transcript analysis
  - Flow cytometry
  - Immunofluorescence
  - Western blotting
  - Dithizone (DTZ) staining
  - Hematoxylin and eosin staining (H & E)
  - ELISA (Enzyme-Linked Immunosorbent assay)
  - Quantification of pancreatic β - Cell related parameters in mice pancreatic sections
- QUANTIFICATION AND STATISTICAL ANALYSIS

SUPPLEMENTAL INFORMATION

Supplemental information can be found online at https://doi.org/10.1016/j.isci.2023.106771.

ACKNOWLEDGMENTS

This study was supported by grants from Indian Council of Medical Research, India (No. 5/4/5-5/Diab/21-NCD-III) to A.K. Flag-HA-USP1 was a gift from Wade Harper (Addgene plasmid#22596) and pLV-TetO-ID2 was a gift from Hubert Schorle (Addgene plasmid #70764). We thank AK lab members for their technical help, suggestions, and encouragement.

AUTHOR CONTRIBUTIONS

Conceptualization, M.F., J.P., and A.K.; Methodology and Formal Analysis, M.F., S.B., S.K., P.S., and A.K.; Investigation, M.F., S.B., and A.K.; Writing – Original Draft, M.F. and A.K.; Writing – Review & Editing, M.F., S.B., J.P., and A.K.; Supervision, A.K.; Funding Acquisition, A.K.

DECLARATION OF INTERESTS

The authors declare no competing. The authors of the above noted article, Anujith Kumar and Meenal Francis have filed certain aspects of this work for patenting.

INCLUSION AND DIVERSITY

We support inclusive, diverse, and equitable conduct of research.

Received: October 21, 2022
Revised: March 8, 2023
Accepted: April 24, 2023
Published: April 26, 2023

REFERENCES

1. Mellitus, D.; American Diabetes Association (2005). Diagnosis and classification of diabetes mellitus. Diabetes Care *28*, S37–S42. https://doi.org/10.2337/diacare.28.suppl_1.s37.

2. Eizirik, D.L., Pasquali, L., and Cnop, M. (2020). Pancreatic β- cells in type 1 and type 2 diabetes mellitus: different pathways to failure. Nat. Rev. Endocrinol. *16*, 349–362. https://doi.org/10.1038/s41574-020-0355-7.

3. Moin, A.S.M., and Butler, A.E. (2019). Alterations in beta cell identity in type 1 and type 2 diabetes. Curr. Diab. Rep. *19*, 83–92. https://doi.org/10.1007/s11892-019-1194-6.

4. Efrat, S. (2019). Beta-cell dedifferentiation in type 2 diabetes: concise review. Stem Cell. *37*, 1267–1272. https://doi.org/10.1002/stem.3059.

5. Nimkulrat, S.D., Bernstein, M.N., Ni, Z., Brown, J., Kendziorski, C., and Blum, B. (2021). The Anna Karenina model of β-cell maturation in development and their dedifferentiation in type 1 and type 2 diabetes. Diabetes *70*, 2058–2066. https://doi.org/10.2337/db21-0211.

6. Shapiro, A.M., Lakey, J.R., Ryan, E.A., Korbutt, G.S., Toth, E., Warnock, G.L., Kneteman, N.M., and Rajotte, R.V. (2000). Islet transplantation in seven patients with type 1 diabetes mellitus using a glucocorticoid-free immunosuppressive regimen. N. Engl. J. Med. *343*, 230–238. https://doi.org/10.1056/nejm200007273430401.

7. Sutherland, D.E.R., Gruessner, R., Kandswamy, R., Humar, A., Hering, B., and Gruessner, A. (2004). Beta-cell replacement therapy (pancreas and islet transplantation) for treatment of diabetes mellitus: an integrated approach. Transplant. Proc. *36*, 1697–1699. https://doi.org/10.1016/j.transproceed.2004.06.069.

8. Kaiser, N., Corcos, A.P., Tur-Sinai, A., Ariav, Y., and Cerasi, E. (1988). Monolayer culture of adult rat pancreatic islets on extracellular matrix: long term maintenance of differentiated B-cell function. Endocrinology *123*, 834–840. https://doi.org/10.1210/endo-123-2-834.

9. Hayek, A., Lopez, A.D., and Beattie, G.M. (1989). Enhancement of pancreatic islet cell monolayer growth by endothelial cell matrix and insulin. In Vitro Cell. Dev. Biol. *25*, 146–150. https://doi.org/10.1007/bf02626171.

10. Hayek, A., Beattie, G.M., Cirulli, V., Lopez, A.D., Ricordi, C., and Rubin, J.S. (1995). Growth factor/matrix-induced proliferation of human adult beta-cells. Diabetes *44*, 1458–1460. https://doi.org/10.2337/diab.44.12.1458.

11. Gershengorn, M.C., Hardikar, A.A., Wei, C., Geras-Raaka, E., Marcus-Samuels, B., and Raaka, B.M. (2004). Epithelial-to-mesenchymal transition generates proliferative human islet precursor cells. Science *306*, 2261–2264. https://doi.org/10.1126/science.1101968.

12. Russ, H.A., Bar, Y., Ravassard, P., and Efrat, S. (2008). In vitro proliferation of cells derived from adult human -cells revealed by cell-lineage tracing. Diabetes *57*, 1575–1583. https://doi.org/10.2337/db07-1283.

13. Russ, H.A., Ravassard, P., Kerr-Conte, J., Pattou, F., and Efrat, S. (2009). Epithelial-mesenchymal transition in cells expanded *in vitro* from lineage-traced adult human pancreatic beta cells. PLoS One *4*, e6417. https://doi.org/10.1371/journal.pone.0006417.

14. Talchai, C., Xuan, S., Lin, H.V., Sussel, L., and Accili, D. (2012). Pancreatic β cell dedifferentiation as a mechanism of diabetic β cell failure. Cell *14*, 1223–1234. https://doi.org/10.1016/j.cell.2012.07.029.

15. Xiao, X., Fischbach, S., Zhang, T., Chen, C., Sheng, Q., Zimmerman, R., Patnaik, S., Fusco, J., Ming, Y., Guo, P., et al. (2017). SMAD3/Stat3 signaling mediates β-cell epithelial-mesenchymal transition in chronic pancreatitis–related diabetes. Diabetes *66*, 2646–2658. https://doi.org/10.2337/db17-0537.

16. Bensellam, M., Jonas, J.-C., and Laybutt, D.R. (2018). Mechanisms of β-cell dedifferentiation in diabetes: recent findings and future research directions. J. Endocrinol. *236*, 109–143. https://doi.org/10.1530/joe-17-0516.

17. Kitamura, Y.I., Kitamura, T., Kruse, J.P., Raum, J.C., Stein, R., Gu, W., and Accili, D. (2005). FoxO1 protects against pancreatic β cell failure through NeuroD and MafA induction. Cell Metab. *2*, 153–163. https://doi.org/10.1016/j.cmet.2005.08.004.

18. Fiori, J.L., Shin, Y.K., Kim, W., Krzysik-Walker, S.M., González-Mariscal, I., Carlson, O.D., Sanghvi, M., Moaddel, R., Farhang, K., Gadkaree, S.K., et al. (2013). Resveratrol prevents β-cell dedifferentiation in

nonhuman primates given a high-fat/high-sugar diet. Diabetes *62*, 3500–3513. https://doi.org/10.2337/db13-0266.

19. Jazurek-Ciesiolka, M., Janikiewicz, J., Dobrzyn, P., Dziewulska, A., Kozinski, K., and Dobrzyn, A. (2019). Oleic acid increases the transcriptional activity of FoxO1 by promoting its nuclear translocation and β-catenin binding in pancreatic β-cells. Biochim. Biophys. Acta, Mol. Basis Dis. *1865*, 2753–2764. https://doi.org/10.1016/j.bbadis.2019.06.018.

20. Rukstalis, J.M., and Habener, J.F. (2007). Snail2, a mediator of epithelial-mesenchymal transitions, expressed in progenitor cells of the developing endocrine pancreas. Gene Expr. Patterns *7*, 471–479. https://doi.org/10.1016/j.modgep.2006.11.001.

21. López-Avalos, M.D., Duvivier-Kali, V.F., Xu, G., Bonner-Weir, S., Sharma, A., and Weir, G.C. (2006). Evidence for a role of the ubiquitin-proteasome pathway in pancreatic islets. Diabetes *55*, 1223–1231. https://doi.org/10.2337/db05-0450.

22. Petroski, M.D. (2008). The ubiquitin system, disease, and drug discovery. BMC Biochem. *9*, S5–S7. https://doi.org/10.1186/1471-2091-9-s1-s7.

23. Hartley, T., Brumell, J., and Volchuk, A. (2009). Emerging roles for the ubiquitin-proteasome system and autophagy in pancreatic β-cells. Am. J. Physiol. Endocrinol. Metab. *296*, E1–E10. https://doi.org/10.1152/ajpendo.90538.2008.

24. Sun-Wang, J.L., Yarritu-Gallego, A., Ivanova, S., and Zorzano, A. (2021). The ubiquitin-proteasome system and autophagy: self-digestion for metabolic health. Trends Endocrinol. Metab. *32*, 594–608. https://doi.org/10.1016/j.tem.2021.04.015.

25. Banno, A., Garcia, D.A., van Baarsel, E.D., Metz, P.J., Fisch, K., Widjaja, C.E., Kim, S.H., Lopez, J., Chang, A.N., Geurink, P.P., et al. (2016). Down regulation of 26S proteasome catalytic activity promotes epithelial-mesenchymal transition. Oncotarget *7*, 21527–21541. https://doi.org/10.18632/oncotarget.7596.

26. Voutsadakis, I.A. (2012). The ubiquitin-proteasome system and signal transduction pathways regulating epithelial mesenchymal transition of cancer. J. Biomed. Sci. *19*, 67. https://doi.org/10.1186/1423-0127-19-67.

27. Tsubakihara, Y., and Moustakas, A. (2018). Epithelial-mesenchymal transition and metastasis under the control of transforming growth factor β. Int. J. Mol. Sci. *19*, 3672. https://doi.org/10.3390/ijms19113672.

28. Lingbeck, J.M., Trausch-Azar, J.S., Ciechanover, A., and Schwartz, A.L. (2003). Determinants of nuclear and cytoplasmic ubiquitin-mediated degradation of MyoD. J. Biol. Chem. *278*, 1817–1823. https://doi.org/10.1074/jbc.m208815200.

29. Nandi, D., Tahiliani, P., Kumar, A., and Chandu, D. (2006). The ubiquitin-proteasome system. J. Biosci. *31*, 137–155. https://doi.org/10.1007/bf02705243.

30. Ventii, K.H., and Wilkinson, K.D. (2008). Protein partners of deubiquitinating enzymes. Biochem. J. *414*, 161–175. https://doi.org/10.1042/bj20080798.

31. Estavoyer, B., Messmer, C., Echbicheb, M., Rudd, C.E., Milot, E., and Affar, E.B. (2022). Mechanisms orchestrating the enzymatic activity and cellular functions of deubiquitinases. J. Biol. Chem. *298*, 102198. https://doi.org/10.1016/j.jbc.2022.102198.

32. Claiborn, K.C., Sachdeva, M.M., Cannon, C.E., Groff, D.N., Singer, J.D., and Stoffers, D.A. (2010). Pcif1 modulates Pdx1 protein stability and pancreatic β cell function and survival in mice. J. Clin. Invest. *120*, 3713–3721. https://doi.org/10.1172/jci40440.

33. Sancho, R., Gruber, R., Gu, G., and Behrens, A. (2014). Loss of Fbw7 reprograms adult pancreatic ductal cells into α, δ, and β cells. Cell Stem Cell *15*, 139–153. https://doi.org/10.1016/j.stem.2014.06.019.

34. Itoh, M., Kim, C.H., Palardy, G., Oda, T., Jiang, Y.J., Maust, D., Yeo, S.Y., Lorick, K., Wright, G.J., Ariza-McNaughton, L., et al. (2003). Mind Bomb is a ubiquitin ligase that is essential for efficient activation of Notch signaling by Delta. Dev. Cell *4*, 67–82. https://doi.org/10.1016/s1534-5807(02)00409-4.

35. Horn, S., Kobberup, S., Jørgensen, M.C., Kalisz, M., Klein, T., Kageyama, R., Gegg, M., Lickert, H., Lindner, J., Magnuson, M.A., et al. (2012). Mind bomb 1 is required for pancreatic β-cell formation. Proc. Natl. Acad. Sci. USA *109*, 7356–7361. https://doi.org/10.1073/pnas.1203605109.

36. Zhou, H., Liu, Y., Zhu, R., Ding, F., Cao, X., Lin, D., and Liu, Z. (2018). OTUB1 promotes esophageal squamous cell carcinoma metastasis through modulating Snail stability. Oncogene *37*, 3356–3368. https://doi.org/10.1038/s41388-018-0224-1.

37. Wu, Y., Wang, Y., Lin, Y., Liu, Y., Wang, Y., Jia, J., Singh, P., Chi, Y.I., Dong, C., Wang, C., et al. (2017). Dub3 inhibition suppresses breast cancer invasion and metastasis by promoting Snail1 degradation. Nat. Comm. *8*, 14228–14236. https://doi.org/10.1038/ncomms14228.

38. Cai, J., Li, M., Wang, X., Li, L., Li, Q., Hou, Z., Jia, H., and Liu, S. (2019). USP37 promotes lung cancer cell migration by stabilizing Snail protein via deubiquitination. Front. Genet. *10*, 1324. https://doi.org/10.3389/fgene.2019.01324.

39. Lin, Y., Wang, Y., Shi, Q., Yu, Q., Liu, C., Feng, J., Deng, J., Evers, B.M., Zhou, B.P., and Wu, Y. (2017). Stabilization of the transcription factors slug and twist by the deubiquitinase dub3 is a key requirement for tumor metastasis. Oncotarget *8*, 75127–75140. https://doi.org/10.18632/oncotarget.20561.

40. Francis, M., Bhaskar, S., Vishnuvajhala, S., Prasanna, J., and Kumar, A. (2022). Dynamics of ubiquitination in differentiation and dedifferentiation of pancreatic β-cells: Putative target for diabetes. Curr. Protein Pept. Sci. *23*, 602–618. https://doi.org/10.2174/1389203723666220422092023.

41. Pearson, G., Chai, B., Vozheiko, T., Liu, X., Kandarpa, M., Piper, R.C., and Soleimanpour, S.A. (2018). Clec16a, Nrdp1, and USP8 form a ubiquitin-dependent tripartite complex that regulates β-cell mitophagy. Diabetes *67*, 265–277. https://doi.org/10.2337/db17-0321.

42. Costes, S., Huang, C.J., Gurlo, T., Daval, M., Matveyenko, A.V., Rizza, R.A., Butler, A.E., and Butler, P.C. (2011). β-cell dysfunctional ERAD/ubiquitin/proteasome system in type 2 diabetes mediated by islet amyloid polypeptide–induced UCH-L1 deficiency. Diabetes *60*, 227–238. https://doi.org/10.2337/db10-0522.

43. Li, S., Zheng, H., Mao, A.P., Zhong, B., Li, Y., Liu, Y., Gao, Y., Ran, Y., Tien, P., and Shu, H.B. (2010). Regulation of virus-triggered signaling by OTUB1-and OTUB2-mediated deubiquitination of TRAF3 and TRAF6. J. Biol. Chem. *285*, 4291–4297. https://doi.org/10.1074/jbc.m109.074971.

44. Tyka, K., Jörns, A., Turatsinze, J.V., Eizirik, D.L., Lenzen, S., and Gurgul-Convey, E. (2019). MCPIP1 regulates the sensitivity of pancreatic beta-cells to cytokine toxicity. Cell Death Dis. *10*, 1–7. https://doi.org/10.1038/s41419-018-1268-4.

45. Takkunen, M., Grenman, R., Hukkanen, M., Korhonen, M., García de Herreros, A., and Virtanen, I. (2006). Snail-dependent and -independent epithelial-mesenchymal transition in oral squamous carcinoma cells. J. Histochem. Cytochem. *54*, 1263–1275. https://doi.org/10.1369/jhc.6a6958.2006.

46. Dhawan, S., Dirice, E., Kulkarni, R.N., and Bhushan, A. (2016). Inhibition of TGF-β signaling promotes human pancreatic β-cell Replication. Diabetes *65*, 1208–1218. https://doi.org/10.2337/db15-1331.

47. Liang, Q., Dexheimer, T.S., Zhang, P., Rosenthal, A.S., Villamil, M.A., You, C., Zhang, Q., Chen, J., Ott, C.A., Sun, H., et al. (2014). A selective USP1-UAF1 inhibitor links deubiquitination to DNA damage responses. Nat. Chem. Biol. *10*, 298–304. https://doi.org/10.1038/nchembio.1455.

48. Ramiya, V.K., Maraist, M., Arfors, K.E., Schatz, D.A., Peck, A.B., and Cornelius, J.G. (2000). Reversal of insulin-dependent diabetes using islets generated in vitro from pancreatic stem cells. Nat. Med. *6*, 278–282. https://doi.org/10.1038/73128.

49. Williams, S.A., Maecker, H.L., French, D.M., Liu, J., Gregg, A., Silverstein, L.B., Cao, T.C., Carano, R.A.D., and Dixit, V.M. (2011). USP1 deubiquitinates ID proteins to preserve a mesenchymal stem cell program in osteosarcoma. Cell *146*, 918–930. https://doi.org/10.1016/j.cell.2011.07.040.

50. Wrighton, K.H. (2011). Tumorigenesis: USP1 keeps ID proteins stable. Nat. Rev. Cancer *11*, 757. https://doi.org/10.1038/nrc3158.

51. Ghil, S.H., Jeon, Y.J., and Suh-Kim, H. (2002). Inhibition of BETA2/NeuroD by Id2. Exp. Mol. Med. *34*, 367–373. https://doi.org/10.1038/emm.2002.52.

52. Cole, L., Anderson, M., Antin, P.B., and Limesand, S.W. (2009). One process for

pancreatic β-cell coalescence into islets involves an epithelial–mesenchymal transition. J. Endocrinol. *203*, 19–31. https://doi.org/10.1677/joe-09-0072.

53. Gouzi, M., Kim, Y.H., Katsumoto, K., Johansson, K., and Grapin-Botton, A. (2011). Neurogenin3 initiates stepwise delamination of differentiating endocrine cells during pancreas development. Dev. Dyn. *240*, 589–604. https://doi.org/10.1002/dvdy.22544.

54. De Jesus, D.S., Mak, T.C.S., Wang, Y.-F., von Ohlen, Y., Bai, Y., Kane, E., Chabosseau, P., Chahrour, C.M., Distaso, W., Salem, V., et al. (2021). Dysregulation of the Pdx1/Ovol2/Zeb2 axis in dedifferentiated β-cells triggers the induction of genes associated with epithelial–mesenchymal transition in diabetes. Mol. Metab. *53*, 101248. https://doi.org/10.1016/j.molmet.2021.101248.

55. Ibrahim, S., Johnson, M., Stephens, C.H., Xu, J., Moore, R., Mariani, A., Contreras, C., Syed, F., Mirmira, R.G., Anderson, R.M., and Sims, E.K. (2021). β-Cell pre-mir-21 induces dysfunction and loss of cellular identity by targeting transforming growth factor beta 2 (Tgfb2) and smad family member 2 (Smad2) mRNAs. Mol. Metab. *53*, 101289. https://doi.org/10.1016/j.molmet.2021.101289.

56. Xie, Y., Avello, M., Schirle, M., McWhinnie, E., Feng, Y., Bric-Furlong, E., Wilson, C., Nathans, R., Zhang, J., Kirschner, M.W., et al. (2013). Deubiquitinase FAM/USP9X interacts with the E3 ubiquitin ligase SMURF1 protein and protects it from ligase activity-dependent self-degradation. J. Biol. Chem. *288*, 2976–2985. https://doi.org/10.1074/jbc.m112.430066.

57. Dexheimer, T.S., Rosenthal, A.S., Luci, D.K., Liang, Q., Villamil, M.A., Chen, J., Sun, H., Kerns, E.H., Simeonov, A., Jadhav, A., et al. (2014). Synthesis and structure–activity relationship studies of N-Benzyl-2-phenylpyrimidin-4-amine derivatives as potent USP1/UAF1 deubiquitinase inhibitors with Anticancer activity against nonsmall cell lung cancer. J. Med. Chem. *57*, 8099–8110. https://doi.org/10.1021/jm5010495.

58. Gorrepati, K.D.D., Lupse, B., Annamalai, K., Yuan, T., Maedler, K., and Ardestani, A. (2018). Loss of deubiquitinase USP1 blocks pancreatic β-cell apoptosis by inhibiting DNA damage response. iScience *1*, 72–86. https://doi.org/10.1016/j.isci.2018.02.003.

59. Prasanna, J., Francis, M., Ashok, A., Ashwathnarayan, A., Banerjee, S., and Kumar, A. (2023). Advancement in understanding the concept of epithelial to mesenchymal transition in pancreatic β-Cells: Implication in diabetes. Curr. Diabetes Rev. *19*. https://doi.org/10.2174/1573399818666220519143414.

60. Mak, T.C., von Ohlen, Y., Wang, Y.F., Kane, E., Jurgaityte, K., Ervilha, P., Chabosseau, P., Distaso, W., Salem, V., Tomas, A., et al. (2019). β-cell dedifferentiation is associated with epithelial-mesenchymal transition triggered by miR-7-mediated repression of mSwi/Snf complex. Preprint at bioRxiv *1*, 789461. https://doi.org/10.1101/789461.

61. Sachs, S., Bastidas-Ponce, A., Tritschler, S., Bakhti, M., Böttcher, A., Sánchez-Garrido, M.A., Tarquis-Medina, M., Kleinert, M., Fischer, K., Jall, S., et al. (2020). Targeted pharmacological therapy restores β-cell function for diabetes remission. Nat. Metab. *2*, 192–209. https://doi.org/10.1038/s42255-020-0171-3.

62. Liu, N., Cai, X., Liu, T., Zou, J., Wang, L., Wang, G., Liu, Y., Ding, X., Zhang, B., Sun, P., et al. (2020). Hypoxia-inducible factor-1α mediates the expression of mature β cell-disallowed genes in hypoxia-induced β cell dedifferentiation. Biochem. Biophys. Res. Comm. *523*, 382–388. https://doi.org/10.1016/j.bbrc.2019.12.063.

63. Maruyama, H., Kleeff, J., Wildi, S., Friess, H., Büchler, M.W., Israel, M.A., and Korc, M. (1999). Id-1 and Id-2 are overexpressed in pancreatic cancer and in dysplastic lesions in chronic pancreatitis. Am. J. Pathol. *155*, 815–822. https://doi.org/10.1016/s0002-9440(10)65180-2.

64. Chakrabarti, L., Wang, B.D., Lee, N.H., and Sandler, A.D. (2013). A mechanism linking Id2-TGFβ crosstalk to reversible adaptive plasticity in neuroblastoma. PLoS One *8*, e83521. https://doi.org/10.1371/journal.pone.0083521.

65. Wang, S., Yan, J., Anderson, D.A., Xu, Y., Kanal, M.C., Cao, Z., Wright, C.V.E., and Gu, G. (2010). Neurog3 gene dosage regulates allocation of endocrine and exocrine cell fates in the developing mouse pancreas. Dev. Biol. *339*, 26–37. https://doi.org/10.1016/j.ydbio.2009.12.009.

66. Premarathne, S., Murtaza, M., Matigian, N., Jolly, L.A., and Wood, S.A. (2017). Loss of Usp9x disrupts cell adhesion, and components of the Wnt and Notch signaling pathways in neural progenitors. Sci. Rep. *7*, 8109–8118. https://doi.org/10.1038/s41598-017-05451-5.

67. Sonego, M., Pellarin, I., Costa, A., Vinciguerra, G.L.R., Coan, M., Kraut, A., D'Andrea, S., Dall'Acqua, A., Castillo-Tong, D.C., Califano, D., et al. (2019). USP1 links platinum resistance to cancer cell dissemination by regulating Snail stability. Sci. Adv. *5*, eaav3235. https://doi.org/10.1126/sciadv.aav3235.

STAR★METHODS

KEY RESOURCES TABLE

REAGENT or RESOURCE	SOURCE	IDENTIFIER
Antibodies		
Pdx1	Abcam	ab47267; RRID:AB_777179
C-peptide	Abcam	ab14181; RRID:AB_300968
USP1	Thermo Fisher Scientific	PA565023; RRID:AB_2662252
E-Cadherin	BD Biosciences	610181; RRID:AB_397580
Actin	Santa Cruz Biotechnology	SC47778; RRID:AB_626632
C-peptide	Cell Signaling Technology	4593; RRID:AB_10691857
Aldh1a3	Abclonal	A15230; RRID:AB_2762125
Insulin	Cloud-Clone Corp.	PAA448Hu01; RRID:AB_2937008
ID2	Abclonal	A0996; RRID:AB_2757515
Anti-Rabbit FITC	Invitrogen	F2765; RRID:AB_2536525
Anti-Mouse FITC	Invitrogen	A11059; RRID:AB_2534106
Anti-Mouse HRP	Invitrogen	62–6520; RRID:AB_2533947
Anti-Rabbit HRP	Thermo Fisher Scientific	32460; RRID:AB_1185567
Anti-mouse 488	Thermo Fisher Scientific	A21042; RRID:AB_2535711
Anti-Rabbit 568	Life Tech	A10042; RRID:AB_2534017
Anti-Mouse 594	Invitrogen	A11005; RRID:AB_2534073
Oligonucleotides		
Primers for PCR, Refer Table S1	This Paper	N/A
Recombinant DNA		
Usp1sh RNA	Sigma Aldrich Co.	TRCN0000030769
pLKO scr	Addgene	pLKO.1 puro; Plasmid:8453
USP1 over expression	Addgene	Flag-HA-USP1; Plasmid: 22596
Id2sh RNA	Addgene	TET-pLKO.1 PURO shId2 #2; Plasmid: 83090
Id2 over expression	Addgene	pLV-tetO-Id2; Plasmid: 70764

RESOURCE AVAILABILITY

Lead contact

Further information and requests for resources and reagents should be directed to and will be fulfilled by the lead contact, Anujith Kumar: anujith.kumar@manipal.edu.

Materials availability

No unique reagents were generated in this project.

Data and code availability

- All data generated in this study is published in the article and supplementary information
- This paper does not report original code
- The data that support the findings of this study are available from the Lead contact on reasonable request

EXPERIMENTAL MODEL AND SUBJECT DETAILS

Animals

All animal experiments were conducted post approval by the Animal Ethics Committee of Manipal Academy of Higher Education (MAHE) (IAEC/KMC/70/2020)). Animals were obtained from Central Animal

House Facility, MAHE, Manipal. For *in vivo* experiments Swiss Albino male mice (10-12-week of age 30-35g of body weight) (N = 20) were used. To isolate endogenous islets Swiss Albino male mice (4-5-week of age 14-16g of body weight) (N = 20) were used. The animals were euthanized by cervical dislocation. All animals were handled in accordance with the national ethical norms, and they were maintained in a facility compliant to national regulations.

Cell culture

MIN6 (National Center for Cell Science, Cell repository, Pune, India) and HEK293T (Kind gift from Prof. Catherine Verfaillie, Leuven) cells were maintained in DMEM HG media (Gibco, 11965-092) containing 10% FBS (Gibco 10270-106), 2 mM Glutamax (Gibco, A12860), Penicillin 100units/ml and Streptomycin 100 μg/ml (Gibco, 15140-122). For dedifferentiation of MIN6 cells, the cells were trypsinized with 0.25% trypsin (Sigma Aldrich, T4049), counted and plated at the rate of 2×10^5 cells/35 mm dish and factors added the following day. The cells were cultured with and without 20 ng TGFβ (Sino Biologicals, 10804-HNAC) & 50 nM proteasome inhibitor (PI) MG132 (Sigma Aldrich, M7449), ML323 (Sigma Aldrich, SML1177) and maintained for 4 days and later harvested for analysis. Handpicked endogenous islets were plated on 10 μg/ml fibronectin (Sigma Aldrich, F1056) coated wells and maintained in RPMI media (Gibco, 11875-093) containing 10% FBS, 2 mM Glutamax, Penicillin 100units/ml and Streptomycin 100 μg/ml with or without 20 ng TGFβ for 4 days and later harvested for analysis.

METHOD DETAILS

Mouse endogenous islet isolation

Pancreas from 2 mice were isolated and digested for 20 min at 37°C in a shaker incubator in digesting enzyme liberase (Sigma Aldrich). The digest was neutralized with 1X HBSS (Sigma Aldrich) and the pellet was subjected to Dextran (Sigma Aldrich) based gradient centrifugation and the top most layer was separated and isolated islet clusters were handpicked using a Nikon SMZ1500 dissection microscope.

Blood glucose tests

Mice was restrained in a tube with tail left out. With a lancet needle prick a droplet of blood was drawn and applied onto glucometer strips and blood glucose concentration was obtained through the glucometer reading (Accu-Chek) in mg/dl.

Glucose tolerance test (GTT)

16 h starved mouse were injected intra-peritoneally with glucose (HiMedia) 2 g/kg body mass and blood glucose levels monitored at 0 min, 15^{th} min, 30^{th} min, 60^{th} min and 120^{th} min. The readings were graphically represented in line graph.

STZ mouse diabetic model and ML323 treatment

With single hand restrain mice starved for 6 h were administered intra-peritoneally with 50 mg/kg body weight of streptozotocin (Sigma Aldrich) for 6 consecutive days. Along with normal and STZ treated conditions, two conditions of ML323 (Sigma Aldrich) treatment were maintained, a) daily treatment of ML323 6 days post STZ treatment and b) treatment of ML323 beginning 3-day prior to STZ treatment. ML323 administered at the rate of 15 μg–30μg/dose.

Transfection and transduction

HEK293T3 Cells were plated at the rate of 3×10^6 cells per 60 mm dish a day prior to transfection. Transfection agent X-tremeGENE (Merck) was added to optiMEM media (Gibco) at the rate of 1:4 ratio of plasmid concentration, vortexed and incubated for 10 min at room temperature. To the transfection mix, the defined concentration of viral packaging plasmids VSV-G and GAG-POL for overexpressing USP1 and ID2 and PMD2G and PsPAX2 packaging plasmid for expressing USP1 shRNA and ID2 shRNA, were added and incubated for 30 min at room temperature. Following which the mixture was added to the HEK293T3 cells and incubated at 37°C in CO2 incubator. The culture supernatant containing the viral particles were collected after 48hrs and 72 h and were concentrated by incubating in PEG with a final concentration of 50% on a rocker at 4°C overnight and centrifuged at 1600rpm for 1 h at 4°C. The viral palette was suspended in 200 μL media and added to respective cells for transduction. Post 24hrs 1 μg/ml of puromycin (HiMedia) was added to respective cultures for selection. Transduced cells were further used for respective experiments.

Transcript analysis

RNA was isolated from cultured cells using TriReagent (Sigma Aldrich) in accordance with manufacturer's protocol. Briefly, monolayer cultures were homogenized with TRIReagent to the mixture. 200 μL/mL chloroform was added vortexed for 10 s and centrifuged at 12000g for 10 min at 4°C. The aqueous layer was collected and RNA was precipitated by adding 500 μL of isopropanol per mL TRIReagent and incubated at room temperature for 10min, then centrifuged at 12000g for 10 min at 4°C. The RNA pellet obtained was washed with 75% ethanol by centrifuging at 7500g for 5 min at 4°C. After which the supernatant was discarded and the pellet air-dried and suspended in DNAse/RNase free water. RNA was quantified using Naodrop and 1 μg RNA was used for cDNA synthesis using commercial cDNA preparatory kit (Takara 6110A). For gene analysis the cDNA was amplified using gene specific primers by qPCR with Takara 2X SYBR Green Mix (Takara RR420A) and analyzed in real-time PCR machine (7500 Applied Biosystems). Gene expression was normalized to the expression of housekeeping gene and the relative fold change was calculated using the 2 -ΔΔCt method. List of primers is provided in Table S1.

Flow cytometry

Cells to be analyzed were trypsinized and washed with 1X PBS and fixed by suspending in 4% Paraformaldehyde (PFA) and incubating at 4ºC overnight. For flow cytometry analysis, the cells were counted and equal number of cells distributed into flow tubes, washed and permeabilized with 1X BD Permwash (BD). The cells were incubated with primary antibody overnight, followed by washes and incubation with secondary antibody for 1 h again washed and re-suspended in FACS buffer for analysis using BD LSR II or BD FACS Caliber.

Immunofluorescence

Cells were fixed with 4% PFA and incubated at 4°C. For the experiment, the cells were washed with 1X PBS, then permeabilized with 0.2% Triton X-100 in PBS for 15 min at RT, blocked in blocking buffer containing 3% BSA in 1X PBS Solution at RT for 1h. Antibodies were diluted in blocking buffer and cells were incubated with the primary antibody at 4°C overnight. The cells were subsequently washed with 0.05% PBST and stained with secondary antibody for 1 h at RT and counterstained with DAPI (1:10000) (Life Technologies) for 1 min and observed under fluorescent microscope Nikon Eclipse TE2000U.

Western blotting

Cells were harvested and lysed with ice-cold RIPA lysis buffer with freshly added protease inhibitor cocktail (Sigma Aldrich, Bangalore). The lysate was spun down at 12000 rpm for 15min and the supernatant collected and stored in −20°C until further use. 100 μg of protein was denatured by heating at 95°C with protein loading buffer and resolved using 10% SDS-Polyacrylamide gel. The resolved proteins were transferred onto charged PVDF membrane (Millipore) using semi-dry blotting apparatus. The membrane was blocked using 3% skimmed milk in 1x TBST. The blots were probed with primary antibody and incubated overnight at 4°C on a rocker. Following day, the blots were washed trice with 1X TBST and incubated with HorseRadish Peroxidase (HRP)-conjugated secondary antibody for 1 h at room temperature on a rocker. The blots were then washed trice with 1X TBST. The blots were developed using Western Bright HRP substrate (Advansta) and imaged on LI-COR C digit blot scanner.

Dithizone (DTZ) staining

10 mg/ml DTZ (Sigma Aldrich) solution was added onto freshly handpicked mouse endogenous islets and incubated for 3–5 min. The stain removed and islets washed with 1X HBSS and phase contrast colored pictures of red stained islets were captured on Nikon Eclipse TE2000U.

Hematoxylin and eosin staining (H & E)

The fixed tissues were embedded in paraffin and 5 μm sections were stained by H & E staining. The sections were deparaffinised with Xylene washes, rehydrated with gradient alcohol washes, the slides were stained with hematoxylin for 1 min and post a 70% alcohol wash stained with Eosin stain for 1 min. The slides were then processed through graded alcohols and xylene and mounted with DPX and subsequently observed using a phase contrast microscope Nikon Eclipse 80i.

ELISA (Enzyme-Linked Immunosorbent assay)

Serum from mice of all experimental conditions were collected and insulin levels were measured following user guide (10-1249-01 Mercodia Ultrasensitive Mouse Insulin Elisa KIT). The OD were read on Perkin Elmer multi-mode spectrophotometer at 540 nm, values were plotted against standard curve, and concentration of serum insulin was calculated.

Quantification of pancreatic β - Cell related parameters in mice pancreatic sections

Whole pancreas from all conditions of 3-independent experiments were considered for each parameter. The average value from 15 random 5-microns histological sections of each pancreas into five consecutive sections of 200 μm apart were analyzed.

β - Cell mass (mg)

β-cell mass was calculated by measuring the ratio of C-PEPTIDE positive area and pancreatic tissue area and multiplied with the weight of the pancreas.

β - Cell volume (mm3)

β-cell volume was calculated by multiplying total insulin positive area with the distance between the sections.

β – Cell count

β-cell number in islets was calculated using ImageJ software using C-PEPTIDE positive cells. ITCN plugin was installed to serve the purpose of automated counting of cell nuclei.

Immunohistochemistry

Paraffin embedded sections were deparaffinized by placing the slides in a 65°C hot plate for 30 s to 1 min followed by xylene washes and rehydrated with gradient alcohols. The sections were subjected to antigen retrieval by 20min incubation in boiling in 10 mM citrate buffer pH 6.0. Blocking with 5% normal serum +1% BSA in 0.05M Tris Hcl buffer pH 7.5 for 1h. Washed in Tris Hcl buffer and added primary antibody and incubated overnight. Following day washed in Tris Hcl buffer twice and incubated with fluorescent secondary antibody overnight and counter stained with DAPI, mounted with mounting media and observed under Nikon TE80i.

QUANTIFICATION AND STATISTICAL ANALYSIS

Student's *t* test was used to analyze the difference between the test cells and its respective controls. The values with $p < 0.05$ were considered statistically significant indicated as * and those with $p < 0.001$ were considered highly significant indicate as **.